Speckle Evolution of Diffusive and Localized Waves

Sheng Zhang,[1] Bing Hu,[1] Patrick Sebbah,[1,2] and Azriel Z. Genack[1]

[1]*Department of Physics, Queens College, The City University of New York, Flushing, New York 11365, USA*

[2]*Laboratoire de Physique de la Matière Condensée/CNRS, Université de Nice–Sophia Antipolis, Parc Valrose, 06108, Nice Cedex 02, France*

(Received 14 November 2006; revised manuscript received 14 April 2007; published 6 August 2007)

We show that while the statistics of static speckle patterns are generic, fluctuations in the change within speckle patterns are greatly enhanced in the localization transition. The probability distributions of the displacement of phase singularities and the standard deviations of the changes of phase and intensity with frequency shift of incident microwave radiation are given in terms of the same expression which describes the probability distribution of total transmission. This function depends only upon a single parameter, the variance of the corresponding variable. The changing statistics in the localization transition reflects the number of underlying electromagnetic modes with which the incident wave interacts.

DOI: 10.1103/PhysRevLett.99.063902 PACS numbers: 42.25.Dd, 42.25.Bs, 42.30.Ms

The superposition of randomly phased waves scattered from a disordered region gives rise to a speckled intensity pattern and a random probability distribution of phase [1]. Nevertheless, the pattern of phase variation is not devoid of structure. A network of vortices of phase and current circulation appears about points of vanishing intensity [2–6] through which the phase jumps by π radians along any line. Measurement of circular current contours and the phase variation in the vicinity of a single phase singularity are shown in Fig. 1(a). Though phase singularities occur at points of darkness, they are robust structures which are present in all scattered wave fields with statistics that are not changed by perturbations of the scattering system. The evolution of the speckle pattern is tied to the motion of phase singularities. Recently, Berry and Dennis [5] calculated the probability distribution of the velocity of singularities for ergodic wave fields produced by the superposition of randomly phased plane waves. Ergodicity is increasingly violated, however, in the Anderson transition from extended diffusing waves to exponentially peaked localized waves [7–9] as a result of enhanced transmission fluctuations [10–15]. The question arises as to whether the statistics of the speckle pattern and its evolution are universal or rather reflect the changing character of radiation in the Anderson transition.

In this Letter, we describe the statistics of evolution of the speckle pattern of transmitted radiation induced by a frequency shift of incident microwave radiation for diffusive and localized waves. We consider three quantities that characterize different aspects of the change in speckle patterns. These are the average displacement of singularities R, and the standard deviations of the phase change and the fractional intensity change, $\sigma_{\Delta\varphi}$ and $\sigma_{\Delta I'}$, respectively. Fluctuations of all these quantities are greatly enhanced for localized waves. Remarkably, the probability distributions for the above variables normalized by the corresponding average over the random ensemble, $\tilde{R}$, $\tilde{\sigma}_{\Delta\varphi}$, and $\tilde{\sigma}_{\Delta I'}$, have the same functional form. This function is the same as for the probability distribution of the total transmission coefficient for a specific incident transverse wave a, normalized by its average value over a collection of random sample configurations, $P(s_a = T_a/\langle T_a\rangle)$. The probability distributions for the parameters marking the change in the speckle pattern are each determined by a single parameter, the variance of the corresponding variable. A comparison of spectra of $\tilde{R}$, $\tilde{\sigma}_{\Delta\varphi}$, and $\tilde{\sigma}_{\Delta I'}$, with transmission spectra indicates that speckle evolution reflects the interaction with the underlying electromagnetic modes of the medium.

The nature of wave propagation is determined by the closeness to the localization threshold. Localization is intimately connected to enhancements of fluctuations of transmission quantities such as the intensity, total transmission, and conductance over the prediction for Gaussian fields and with the correlation of these variables with varying voltage [10], sample structure [16], frequency [17], scattering angle [11,18], and position [19]. The localization threshold, which corresponds to the point at which the dimensionless ratio of the width of modes to their spacing is unity [8], occurs at $\mathrm{var}(s_a) = 2/3$ [14]. Measurement of microwave speckle are described below for diffusive and localized waves, with $\mathrm{var}(s_a) = 0.14$ and 3.0, respectively.

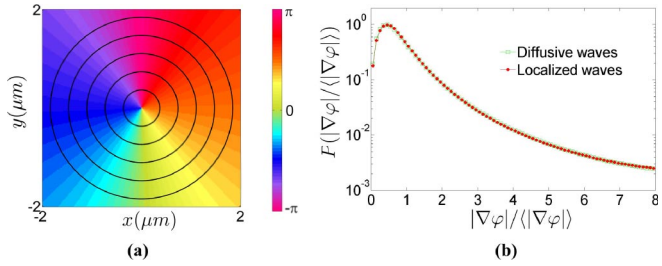

FIG. 1 (color online). (a) Phase map and contours of magnitude of current near a phase singularity. The value of phase is represented by the color (or shade) defined in the bar. (b) Probability distributions of the magnitude of phase gradient normalized by its ensemble average.

The electromagnetic field transmitted through the scattering medium contained in a copper tube is picked up by a short wire antenna. The amplitude $|E|$ and phase shift φ of the field polarized along the antenna relative to the incident field is detected with use of a vector network analyzer. The sample is composed of alumina spheres with diameter 0.95 cm and refractive index 3.14 which are embedded in Styrofoam shells of refractive index 1.04 to produce an alumina volume fraction of 0.068. Photons are localized in a narrow window above the first Mie resonance [20]. Spectra are taken on a 1-mm-square grid over the output face. Speckle patterns were obtained for diffusive waves from 14.7 to 15.7 GHz and for localized waves from 10 to 10.24 GHz in 40 random configurations [20]. Spectra were taken with frequency steps of 625 kHz for diffusive waves and 300 kHz for localized waves, corresponding to approximately $1/7$ of the field correlation frequency [17] in each case. New realizations of the random sample were created once the full speckle pattern is recorded by rotating and vibrating the sample tube.

Since the measured speckle patterns are generated with monochromatic waves, the bandwidth of the power spectrum in k space is limited by the magnitude of the wave vector $k = 2\pi/c$, i.e., $-k < k_x, k_y < k$. According to the two-dimensional sampling theorem [21], the full field in a 2D space can be obtained once the sampling resolution on the plane is higher than the critical value $(1/2k) \times (1/2k)$, which is 1.52×1.52 mm^2 for 15.7 GHz and 2.33×2.33 mm^2 for 10.24 GHz waves. Our measurements on a 1-mm-square grid are therefore sufficiently dense to reconstruct the speckle pattern with arbitrarily high resolution. Applying this theorem reveals the current vortex structure surrounding the phase singularity in the circular contours of current magnitude, $J = I|\nabla\varphi|$ [5], shown in Fig. 1(a) which were also observed in optical transmission through sandblasted glass [6].

To test whether the statistics within speckle patterns are generic, we compare the probability distributions of the magnitude of the phase gradient normalized by its ensemble average value, $P(|\nabla\varphi|/\langle|\nabla\varphi|\rangle)$, for diffusive and localized waves. The close correspondence of these distributions seen in Fig. 1(b) demonstrates that the statistics of phase variation within speckle patterns are universal.

Next we consider whether changes between speckle patterns are similarly generic. The difference between the evolution of the speckle pattern as the frequency is scanned for diffusive and localized waves can be seen directly in the movie clips of [22]. The motion of singularities is relatively uniform for diffusive waves whereas, for localized waves, quiescent periods are punctuated by intervals of rapid motion. This qualitative difference is seen in the plots of $P(\tilde{R})$ shown in Fig. 2. For diffusive waves, the distribution is narrow and peaked near the average value of $\tilde{R}$ of unity, whereas, for localized waves, the peak of $P(\tilde{R})$ is shifted towards lower values while the probability of large displacements is greatly enhanced. Excellent agreement

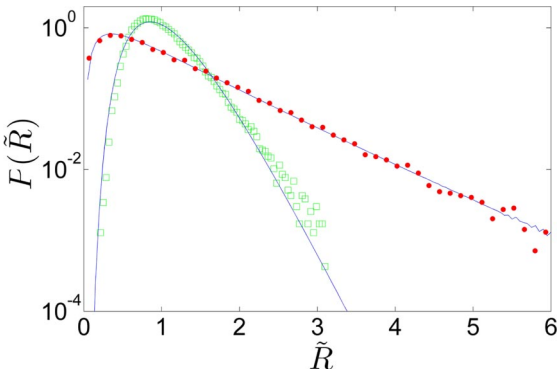

FIG. 2 (color online). Probability distributions of ensemble-average-normalized average displacement of singularities within one speckle pattern $\tilde{R}$ for diffusive [green (light gray) squares] and localized [red (gray) dots] waves. The solid lines are calculated from Eq. (1) based on the measured value of var($\tilde{R}$).

with the measured distributions, $P(\tilde{R})$, is found using an expression,

$$P(x) = \frac{1}{2\pi i}\int_{-i\infty}^{i\infty} \exp(qx) F(3q\beta/2) dq, \tag{1}$$

$$F(q) = \exp\left[-\frac{2\ln^2(\sqrt{(1+q)}+\sqrt{q})}{3\beta}\right], \tag{2}$$

where $\beta = \mathrm{var}(x)$. The variances for localized and diffusive waves are 0.705 and 0.128, respectively. Equations (1) and (2) were first derived for the distribution of s_a in the diffusive limit [13,23], but were found to apply to strongly localized waves as well [14].

In addition to the motion of singularities, the entire speckle pattern evolves as the frequency is scanned. This is illustrated in Fig. 3 by the maps of the change within the speckle pattern in a single frequency step for two cases in which the average singularity displacement is 4 times or one quarter the average displacement. Displacements of the singularity in consecutive frames (circles to stars) are indicated in Figs. 3(a) and 3(d). The phase change $\Delta\varphi_{ij} = \varphi_{ij}(\nu + \Delta\nu) - \varphi_{ij}(\nu)$ and the fractional change in intensity between adjacent frames, $\Delta I'_{ij} = 2[I_{ij}(\nu + \Delta\nu) - I_{ij}(\nu)]/[I_{ij}(\nu + \Delta\nu) + I_{ij}(\nu)]$ at each point (i, j) within the output field, are shown below the corresponding speckle patterns in Fig. 3. The examples shown in Fig. 3 indicate that $\Delta\varphi$ and $\Delta I'$ are largest near phase singularities. This is expected since the phase is singular and the intensity vanishes at the singularity. The figure also suggests that R, and the extent of variation of the changes in the phase and fractional intensity over the speckle pattern are correlated. The variation of the phase changes over all sampled points in the pattern may be characterized by the standard deviations of $\Delta\varphi$,

$$\sigma_{\Delta\varphi} = \sqrt{\frac{1}{N}\sum_{i,j}\left(\Delta\varphi_{ij} - \frac{1}{N}\sum_{p,q}\Delta\varphi_{pq}\right)^2},$$

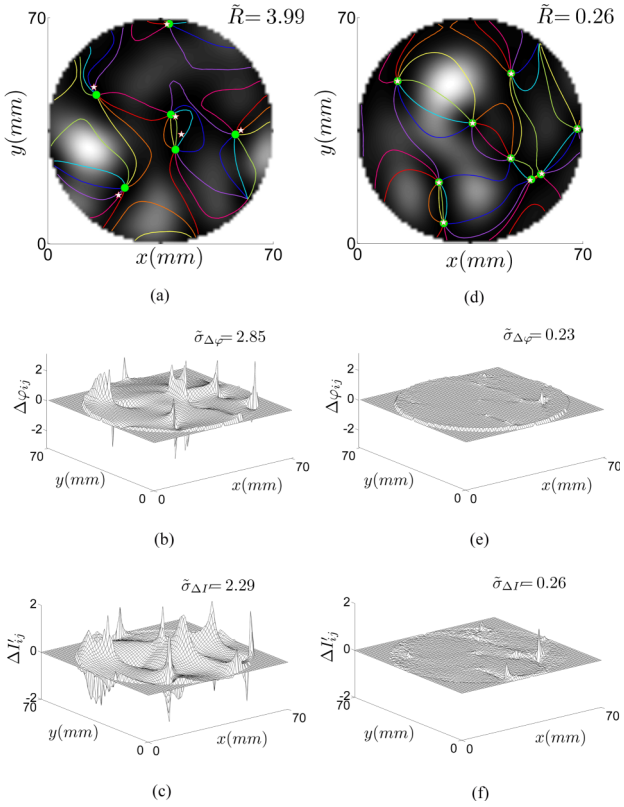

FIG. 3 (color online). Two examples of average displacement of phase singularities [(a) and (d)], phase changes [(b) and (e)], and fractional intensity changes [(c) and (f)] for one step of frequency shift. Colored (shaded) lines in (a) and (d) are equiphase lines with 8 equally spaced values from $-\pi$ to π in colors (shades) defined in the bar in Fig. 1.

where N is the number of sampled points. The standard deviation of the fractional intensity change $\Delta I'$ may be similarly defined. The correlation between these three quantities is confirmed in the linear relation between the ensemble average of the displacement, $\tilde{R}$, and $\tilde{\sigma}_{\Delta\varphi}$ or $\tilde{\sigma}_{\Delta I'}$ shown in Fig. 4, with slopes of 1.03 and 1.02, respectively.

In addition to the proportionality between $\tilde{R}$, $\tilde{\sigma}_{\Delta\varphi}$, and $\tilde{\sigma}_{\Delta I'}$seen in Fig. 4, these indicators of speckle change have similar mesoscopic probability distributions. The distributions for $\tilde{\sigma}_{\Delta\varphi}$ and $\tilde{\sigma}_{\Delta I'}$ shown in Fig. 5 are well fit by Eq. (1) with the variances of these distributions as the fitting parameter. The variances found in the fit for the diffusive and localized case studies are var$(\tilde{\sigma}_{\Delta\varphi}) = 0.057$ and 0.693, and var$(\tilde{\sigma}_{\Delta I'}) = 0.036$ and 0.473. The ratios of the variances for localized and diffusive waves for $\tilde{\sigma}_{\Delta\varphi}$ and $\tilde{\sigma}_{\Delta I'}$ are 12.1 and 13.3, respectively, whereas the ratio of the variances for s_a is 22.7. The smaller value of the corresponding ratio for var$(\tilde{R})$ may be due to the small number of singularities whose displacement is averaged. This broadens the distributions for both diffusive and localized waves.

The source of the broadening of the distributions of these three parameters in the localization transition can be found by comparing typical spectra of these quantities with spectra of total transmission (Fig. 6). Fluctuations of all quantities shown are relatively small for diffusive waves because the incident wave always falls within the linewidth of several electromagnetic modes. In contrast, sharp fluctuations are observed in spectra for localized waves since a distinction can be drawn between being on or off resonance. On resonance, transmission may be dominated by the interaction with a single electromagnetic mode. The speckle pattern then essentially corresponds to the distinctive pattern of the resonant mode. Though the transmission will vary appreciably as the wave is tuned through resonance, the change in the spatial distribution of the field may be imperceptible, since it is dominated by the field pattern of a single mode. Once the frequency is tuned sufficiently far off resonance, however, the spatial distribution of the wave will change since the contribution of the resonant mode may be reduced to the level of the contributions from other modes. The peaks in the spectra of $\tilde{R}$, $\tilde{\sigma}_{\Delta\varphi}$, and $\tilde{\sigma}_{\Delta I'}$

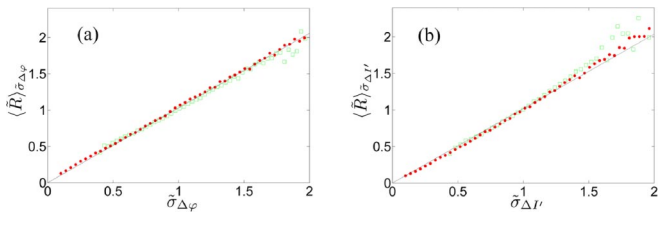

FIG. 4 (color online). (a) Average $\tilde{R}$ for given $\tilde{\sigma}_{\Delta\varphi}$ vs $\tilde{\sigma}_{\Delta\varphi}$; (b) average $\tilde{R}$ for given $\tilde{\sigma}_{\Delta I'}$ vs $\tilde{\sigma}_{\Delta I'}$ for diffusive and localized waves.

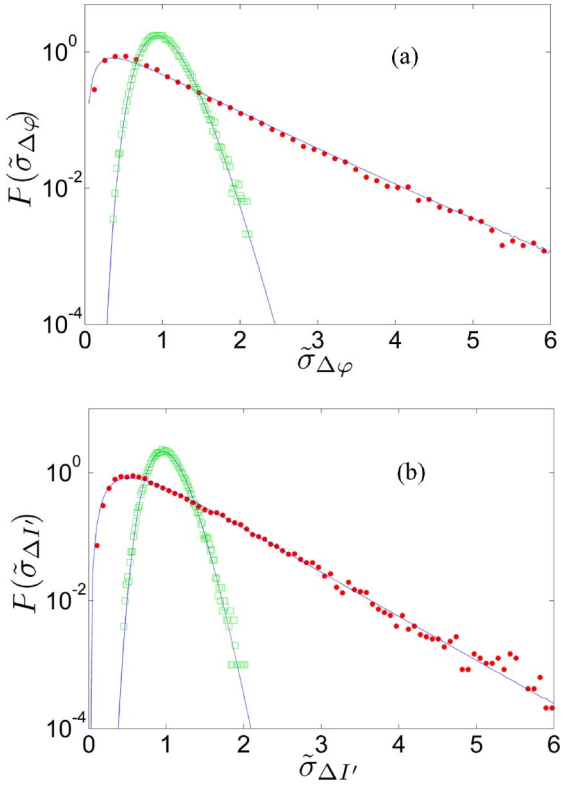

FIG. 5 (color online). Probability distributions of (a) $\tilde{\sigma}_{\Delta\varphi}$ and (b) $\tilde{\sigma}_{\Delta I'}$ for diffusive and localized waves.

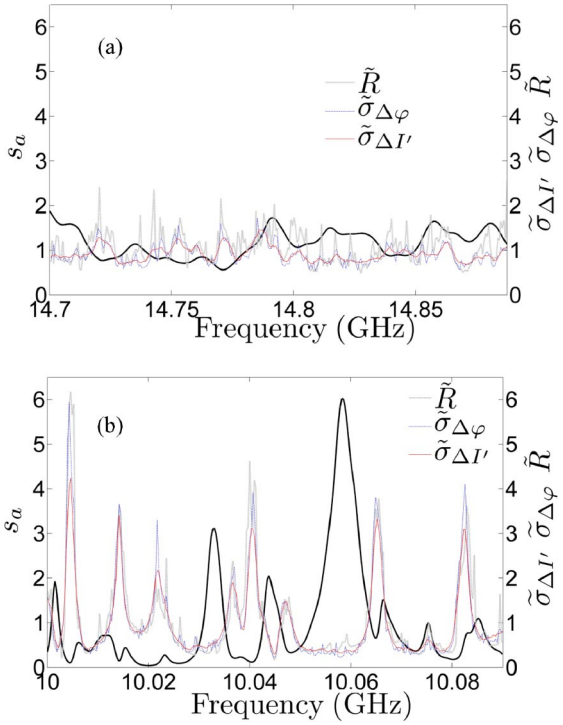

FIG. 6 (color online). Spectra of s_a (black thick lines), $\tilde{R}$, $\tilde{\sigma}_{\Delta\varphi}$, and $\tilde{\sigma}_{\Delta I'}$ for (a) diffusive and (b) localized waves.

are observed between transmission resonances. This is in contrast to the average of the phase derivative with frequency shift over the speckle pattern, which is proportional to the photon dwell time and is peaked on resonance [24].

In conclusion, we have found that the statistics of speckle pattern evolution with frequency shift reflect the localization transition. The three parameters, $\tilde{R}$, $\tilde{\sigma}_{\Delta\varphi}$, and $\tilde{\sigma}_{\Delta I'}$, are strongly correlated and the corresponding probability distributions have the same form as the probability distribution of total transmission. All these functions depend only upon their variance. The similar functional form of the statistics of different aspects of wave propagation and localization reflects an unanticipated unity of mesoscopic phenomena. A comparison of spectra of these parameters shows that the statistics of speckle pattern evolution reflects the degree to which modes overlap spectrally, which is the essence of the localization transition. Thus the variances of $\tilde{\sigma}_{\Delta\varphi}$ and $\tilde{\sigma}_{\Delta I'}$ are measures of the closeness to the localization threshold as are traditional measures, such as the scaling of conductance [7,8] and transmission [17,25], fluctuations of conductance [10,12] and transmission [14,15], long range correlation [11,19] and coherent backscattering [26]. In addition, measurements of changes of speckle patterns with the quantities studied in this Letter may be used to characterize changes in a variety of systems including geological formations, ice caps, and aerospace components, and might be exploited to monitor the heart undergoing cardiac fibrillation [27].

We thank A. A. Chabanov for discussions of localization. This work was supported by the NSF under Grant No. DMR-0538350.

[1] J. W. Goodman, *Statistical Optics* (Wiley, New York, 1985).
[2] J. F. Nye and M. V. Berry, Proc. R. Soc. A **336**, 165 (1974); M. V. Berry, J. Phys. A **11**, 27 (1978).
[3] N. Shvartsman and I. Freund, Phys. Rev. Lett. **72**, 1008 (1994); I. Freund and M. Wilkinson, J. Opt. Soc. Am. A **15**, 2892 (1998).
[4] I. Freund, Waves Random Media **8**, 119 (1998).
[5] M. V. Berry and M. R. Dennis, Proc. R. Soc. A **456**, 2059 (2000).
[6] W. Wang, S. G. Hanson, Y. Miyamoto, and M. Takeda, Phys. Rev. Lett. **94**, 103902 (2005).
[7] P. W. Anderson, Phys. Rev. **109**, 1492 (1958); E. Abrahams, P. W. Anderson, D. C. Licciardello, and T. V. Ramakrishnan, Phys. Rev. Lett. **42**, 673 (1979).
[8] D. J. Thouless, Phys. Rev. Lett. **39**, 1167 (1977).
[9] S. John, Phys. Rev. Lett. **53**, 2169 (1984).
[10] R. A. Webb, S. Washburn, C. P. Umbach, and R. B. Laibowitz, Phys. Rev. Lett. **54**, 2696 (1985).
[11] S. Feng, C. Kane, P. A. Lee, and A. D. Stone, Phys. Rev. Lett. **61**, 834 (1988).
[12] B. L. Altshuler, P. A. Lee, and R. A. Webb, *Mesoscopic Phenomena in Solids* (Elsevier Science, New York, 1991).
[13] M. C. W. van Rossum and Th. M. Nieuwenhuizen, Rev. Mod. Phys. **71**, 313 (1999).
[14] A. A. Chabanov, M. Stoytchev, and A. Z. Genack, Nature (London) **404**, 850 (2000).
[15] M. P. van Albada, J. F. de Boer, and A. Lagendijk, Phys. Rev. Lett. **64**, 2787 (1990).
[16] G. Maret and P. E. Wolf, Z. Phys. B **65**, 409 (1987).
[17] A. Z. Genack, Phys. Rev. Lett. **58**, 2043 (1987).
[18] I. Freund, M. Rosenbluh, and S. Feng, Phys. Rev. Lett. **61**, 2328 (1988).
[19] A. Z. Genack, N. Garcia, and W. Polkosnik, Phys. Rev. Lett. **65**, 2129 (1990).
[20] A. A. Chabanov and A. Z. Genack, Phys. Rev. Lett. **87**, 153901 (2001).
[21] J. W. Goodman, *Introduction to Fourier Optics* (McGraw-Hill, New York, 1968).
[22] See EPAPS Document No. E-PRLTAO-99-005733 for movie clips of speckle pattern changing with frequency. Diff.avi and Loc.avi are for diffusive and localized waves correspondingly. For more information on EPAPS, see http://www.aip.org/pubservs/epaps.html.
[23] E. Kogan and M. Kaveh, Phys. Rev. B **52**, R3813 (1995); Th. M. Nieuwenhuizen and M. C. van Rossum, Phys. Rev. Lett. **74**, 2674 (1995).
[24] A. A. Chabanov and A. Z. Genack, Phys. Rev. Lett. **87**, 233903 (2001).
[25] D. S. Wiersma, P. Bartolini, A. Lagendijk, and R. Righini, Nature (London) **390**, 671 (1997).
[26] D. S. Wiersma, M. P. van Albada, B. A. van Tiggelen, and A. Lagendijk, Phys. Rev. Lett. **74**, 4193 (1995).
[27] R. A. Gray, A. M. Pertsov, and J. Jalife, Nature (London) **392**, 75 (1998).